

## Supplementary Data:

<i>Amino acid</i>	<i>10 mM Glucose</i> <i>Rate</i>	<i>0 mM Glucose</i> <i>Rate</i>
Glutamine	-116 ± 6.7	-121 ± 10.3
Serine	-11.9 ± 0.2	-14.8 ± 2.2
Leucine	-11.7 ± 2.9	-8.4 ± 0.4
Isoleucine	-9.9 ± 2.7	-12.2 ± 3.1
Cystine	-7.2 ± 0.4	-8.3 ± 0.5
Valine	-5.9 ± 2.9	-5.7 ± 0.1
Arginine	-3.8 ± 0.6	-5.0 ± 0.7
Threonine	-3.7 ± 5.6	-3.8 ± 1.9
Lysine	-3.1 ± 2.6	-4.0 ± 0.3
Phenylalanine	-1.7 ± 1.8	-2.0 ± 0.1
Methionine	-1.5 ± 0.7	-1.5 ± 0.1
Tyrosine	-0.8 ± 1.8	-1.6 ± 0.1
Histidine	-0.2 ± 0.9	-1.0 ± 0.1
Citrulline	-0.1 ± 0	-0.1 ± 0.0
Asparagine †	0.0 ± 0	2.4 ± 0.2
Tryptophan	0.7 ± 0.4	-0.2 ± 0.7
α-Aminobutyrate †	0.9 ± 0.2	2.7 ± 0.2
Glycine	1.4 ± 1.9	7.3 ± 0.6
Ornithine †	1.9 ± 0.1	3.6 ± 0.5
Alanine †	25.8 ± 1.1	10.3 ± 0.7
Glutamate	29.3 ± 2.7	36.2 ± 5.2

### Supplementary Table 1: Effect of glucose deprivation on amino acid utilization.

Amino acids are ranked from the most rapidly consumed to the most rapidly secreted.

All rates are in net nmoles consumed (negative values) or secreted (positive)/hr/million cells. Glutamine rates were determined using a chemical analyzer (NOVA Biomedical) and all other rates were measured using high performance liquid chromatography. Each rate was calculated as the average ± SD of three independent cultures. † denotes statistically significant differences (p<0.05).

### **Supplementary Materials and Methods:**

**Measurement of  $^{13}\text{C}$ -Lactate.** L-[3- $^{13}\text{C}$ ]-glutamine was obtained from Isotec, and sodium L-[ $^{13}\text{C}_3$ ]-lactate and sodium L-[3- $^{13}\text{C}$ ]-lactate were obtained from Cambridge Isotope Labs. To measure the  $^{13}\text{C}$  enrichment in lactate, an aliquot of 5  $\mu\text{L}$  of medium was transferred to a glass tube and 17.9 nMoles of an internal standard (sodium L-[ $^{13}\text{C}_3$ ]-lactate) was added. The sample was extracted with 1 mL each of methanol, chloroform and water. After centrifugation at 650 x g for 10 minutes, the aqueous phase was evaporated under air and derivatized at 42°C for 30 minutes in 100  $\mu\text{L}$  Tri-Sil reagent (Thermo Scientific). Standards containing known ratios of unlabeled sodium lactate and sodium L-[3- $^{13}\text{C}$ ]-lactate were prepared using the same method. Derivatized samples were analyzed by GC/MS with an Agilent 6890N GC coupled to an Agilent 5973 Mass Selective Detector. One  $\mu\text{L}$  of derivatized material was used for each standard/sample. The oven temperature was ramped from 70°C to 150°C by 5°C/minute, then by 10°C/minute to 325°C. The abundance of ions of  $m/z$  117 (unenriched), 118 (enriched) and 119 (internal standard) were measured and used to calculate A.P.E. and total lactate abundance.

**Stable GDH knockdown.** Sequences for negative control and GLUD1-A shRNAs were based on the sequences of the negative control and GLUD1-A siRNAs used in Fig. 4. Oligomers were constructed for the shRNA and its complement, annealed and cloned into pLKO.1-TRC (Addgene). These vectors were used to produce lentiviral particles and to infect SF188-xL glioblastoma cells according the manufacturer's protocol. After 36 hours of culture in medium containing polybrene (8  $\mu\text{g}/\text{mL}$ ) and lentiviral particles, the

cells were selected with puromycin (1  $\mu\text{g}/\text{mL}$ ) for 6 days. Pools of puromycin resistant cells were used for the experiments in Figure 4D and Supplementary Figure 5.

### **Supplementary Figure Legends:**

**Supplementary Figure 1:** Acute glucose withdrawal does not affect ATP content of glioblastoma cells. Glioblastoma cells were cultured in the presence or absence of glucose for 8 hours, then cells were lysed and ATP content was measured using a commercial kit (Invitrogen). The average and SD are shown for three independent cultures for each condition.

**Supplementary Figure 2:** Effect of glucose withdrawal on transfer of  $^{13}\text{C}$  from glutamine to lactate. Cells were cultured in L-[3- $^{13}\text{C}$ ]-glutamine and decreasing concentrations of glucose, and the medium was analyzed for the atomic percent enrichment (A.P.E.) of lactate (A) and the total amount of  $^{13}\text{C}$ -labeled lactate (B). The average and SD are shown for three independent cultures for each condition.

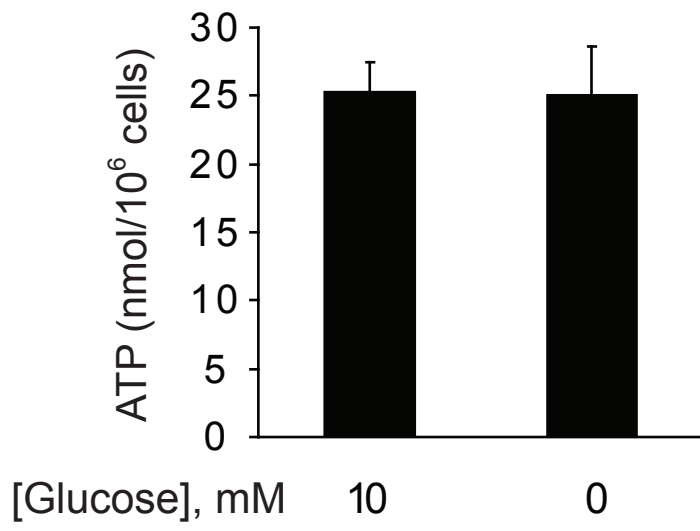
**Supplementary Figure 3:** Glucose deprivation increases GDH activity in mouse embryonic fibroblasts (MEFs). SV40 Large T-immortalized MEFs (0.75 million) were plated into 6-cm dishes and cultured overnight until 90% confluent. The cells were then rinsed with PBS and cultured for 8 hours in medium containing 4 mM L-[ $\alpha$ - $^{15}\text{N}$ ]-glutamine, with or without glucose. Medium was analyzed for glutamine and ammonia

(A). GDH activity (B) was measured as described in the main text. The average and SD are shown for three independent cultures for each condition.

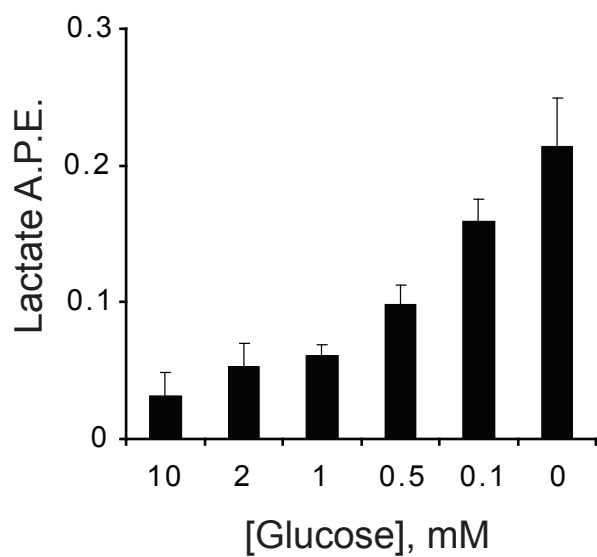
**Supplementary Figure 4:** Dimethyl  $\alpha$ -ketoglutarate suppresses total ammoniogenesis and GDH activity. Glioblastoma cells were cultured in the presence or absence of glucose and dimethyl- $\alpha$ -ketoglutarate (dm- $\alpha$ KG), in medium containing L- $[\alpha$ - $^{15}\text{N}$ ]-glutamine. Total ammonia production and GDH activity were determined for each condition. The average and SD are shown for three independent cultures.

**Supplementary Figure 5:** A glioblastoma cell line with constitutive knockdown of GDH expression. SF188-derived glioblastoma cells stably expressing a negative control shRNA (NC) or an shRNA directed against the *GLUD1* transcript (GLUD1-A) were obtained. These cell lines were examined for GDH protein expression (A), for GDH activity (B), and for loss of viability during glucose withdrawal (C). D, Both cells lines were cultured for 7 hours in medium containing L- $[3$ - $^{13}\text{C}]$ -glutamine, and intracellular metabolites were analyzed by  $^{13}\text{C}$  NMR. The 34 ppm region of each spectrum is enlarged in Figure 4D to emphasize decreased labeling of glutamate C4. The wider regions of the spectra shown here verify that other aspects of metabolism, including labeling in aspartate C2 and C3, were not significantly affected by GDH knockdown.

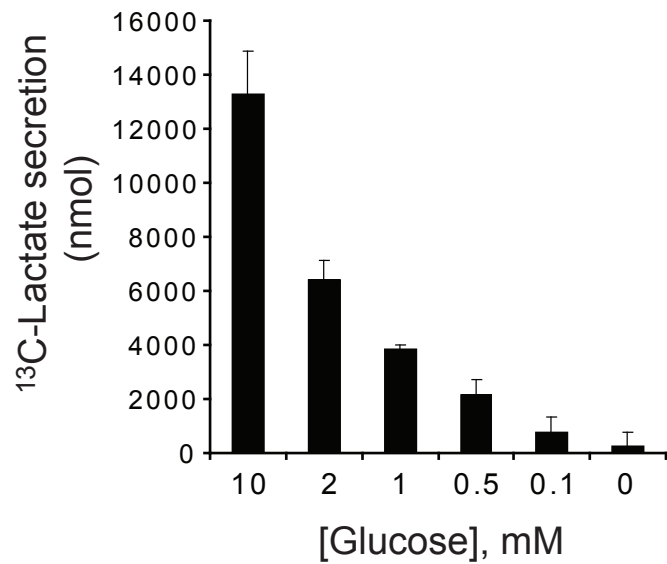
# Yang et al, Supplementary Fig. 1



**A**

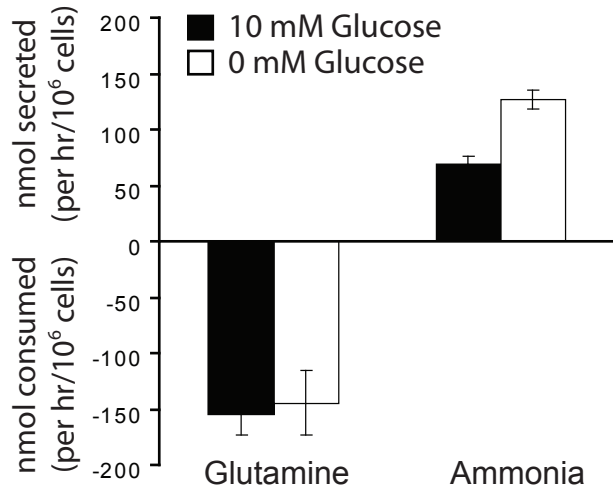


**B**

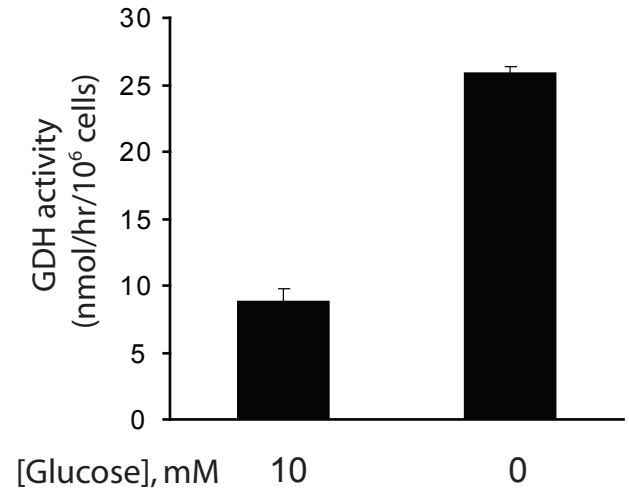


# Yang et al, Supplementary Fig. 3

## A

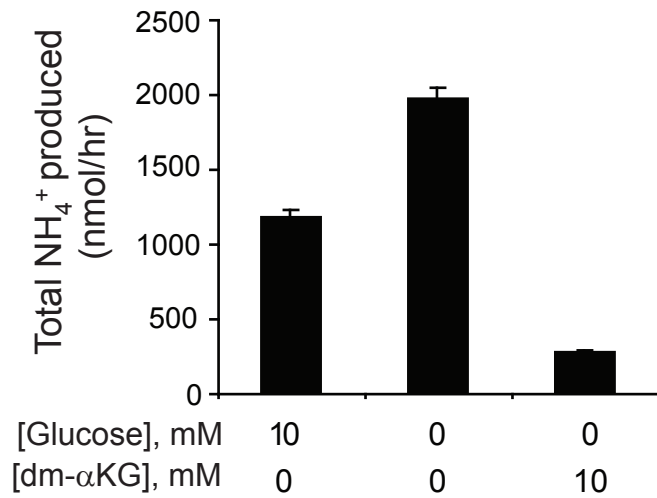


## B

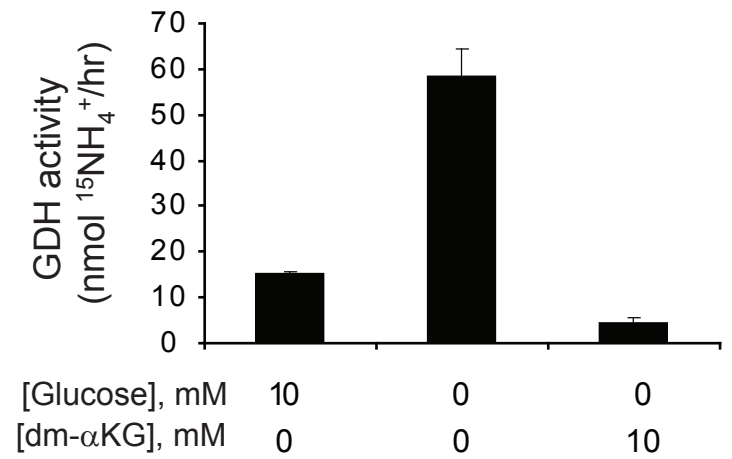


Yang et al, Supplementary Fig. 4

A



B



Yang et al, Supplementary Fig. 5

